PCCP

PAPER

View Article Online
View Journal | View Issue

Cite this: *Phys. Chem. Chem. Phys.*, 2018, **20**, 16477

Understanding the fundamentals of acid-induced ionic liquid-based aqueous biphasic system†

Vijetha Mogilireddy,[a] Matthieu Gras,[a] Nicolas Schaeffer,[b] Helena Passos,[b] Lenka Svecova,[a] Nicolas Papaiconomou,‡[a] João A. P. Coutinho[b] and Isabelle Billard*[a]

Ionic-liquid-based aqueous biphasic systems (IL-based ABS) have demonstrated exceptional performance in bioseparation processes. However, IL-based ABS are of limited interest for metal extraction as most metals are not stable in their neutral or alkaline pH conditions. In the quest for better extraction systems for metals, the development of IL-based ABS with highly acidic solutions (AcABS), induced by the mixture of a hydrophilic IL ($[P_{44414}]Cl$), a mineral acid (HCl, HNO_3 or H_2SO_4) and water, opens new possibilities. A comprehensive investigation of fundamental aspects of IL-based AcABS was performed, including the temperature dependence of the phase diagrams, tie-lines and ion exchange behavior, evidencing the unique characteristics of these new systems. In particular, the favorable biphasic formation with an increase in temperature showcases the lower critical solution temperature (LCST) behavior of the phosphonium-based IL and opens many possibilities for AcABS application by creating stimuli responsive systems. The anion exchange identified highlights the IL-based AcABS complexity that renders the analytical characterization of the phases mandatory, instead of the traditional method coupling an empirical fit of the binodal with the lever-arm rule. Through judicious selection of the inorganic acid, different extraction systems can be obtained by tuning the degree of anion-exchange, underlining the versatility of the proposed AcABS system.

Received 5th May 2018,
Accepted 30th May 2018

DOI: 10.1039/c8cp02862a

rsc.li/pccp

Introduction

Aqueous biphasic systems (ABS) have attracted attention in liquid–liquid bioseparation due to their biocompatibility, and environmentally friendly and safe nature.[1] The common types of ABS are composed of two polymers or a polymer and a salt, and use either the polymer or the salt as a salting-out agent to form two aqueous phases for the separation and purification of proteins, cells, viruses and many other biocompounds.[2,3] However the performance of these systems is limited by the polarity differences between the phases and the viscosity of the polymer-rich phase. In an effort to overcome these limitations and improve the performance of ABS, ionic liquid (IL)-based ABS were first proposed by Rogers and co-workers using imidazolium-based ILs.[4] ILs are salts that melt below 100 °C, and possess many unique properties that allow them to be used with advantage on solvent extraction processes.[5]

Since the discovery of IL-based ABS, efforts have been addressed towards the development of extraction processes making use of the tunability of ILs and concentrated salt aqueous solutions, with pH ranging from slightly acidic to strongly alkaline.[6–8] A large set of literature data has focused on the effect of IL anion and cation nature, salts, pH and temperature on the phase behavior of IL-based ABS.[7,9–12] However, the possibility of using acidic aqueous solutions to prepare ABS was confined to a limited number of studies at relatively high pH values.[6] In the search for better extraction systems for metals, Gras and co-workers[13] developed a novel type of acid induced aqueous biphasic systems (AcABS). In these new systems the inorganic salt commonly used in the formation of the ABS is replaced by an acid,[13] where the authors demonstrated that IL-based AcABS present a thermomorphic behavior and a high potential for application in the simultaneous leaching and extraction of critical metals. However, to be able to design novel AcABS for desired applications, the understanding of the fundamental aspects of these systems must be mastered. ABS typically display weak temperature dependencies, except when prepared with poly(ethylene)glycol (PEG), poly(propylene)glycol (PPG) or non-ionic surfactants. These polymer and surfactant-based ABS exhibit a thermomorphic or thermoreversible behavior where the increase in temperature increases the biphasic region, while other systems may exhibit a upper critical solution temperature

[a] *Univ. Grenoble Alpes, CNRS, Grenoble INP (Institute of Engineering Univ.), LEPMI, 38000 Grenoble, France. E-mail: Isabelle.billard@grenoble-inp.fr*
[b] *CICECO – Aveiro Institute of Materials, Department of Chemistry, University of Aveiro, 3810-193 Aveiro, Portugal*

† Electronic supplementary information (ESI) available. See DOI: 10.1039/c8cp02862a

‡ Current address: Institut de Chimie de Nice, Université Côte d'Azur, Nice, France.

(UCST) like type behavior.[8,11] Anion exchange in conventional liquid–liquid extractions, where the anions from aqueous phase may exchange with those in organic or IL–rich phase, was studied by Dupont *et al.*[14] that established under which conditions this exchange may be relevant or negligible. The knowledge of this ionic exchange is a prerequisite for implementing the recycling of IL at the end of the extraction processes. Despite its importance, very few other studies address the ion exchange in IL-based ABS, often relying on the original results by Gutowski *et al.*[15] reporting that for the limited number of systems studied the ion exchange was not important.

With this aim, this work reports a comprehensive study of a new class of AcABS constituted by the IL tributyltetradecylphosphonium chloride ([P_{44414}]Cl) and different mineral acids (HCl, HNO_3 and H_2SO_4). The thermomorphic nature of the HCl–[P_{44414}]Cl–H_2O system is evaluated by the measurement of the binodals at several temperatures. Due to the unusual shape of IL-based AcABS binodal curves, various empirical equations are here evaluated to describe them. The tie-lines were obtained through direct measurement of the phase compositions. The phase diagrams of AcABS systems with acids HNO_3 and H_2SO_4 are also presented, and in order to be able to take advantage of these systems as extraction platforms, the extent of ion exchange when replacing HCl with other mineral acids, not sharing a common anion with the IL, is investigated.

Materials and methods

Chemicals and instrumentation

The IL [P_{44414}]Cl (tributyltetradecylphosphonium chloride) was obtained from Cytec industries. The mineral acids HCl (37 wt%), H_2SO_4 (96 wt%), and HNO_3 (68 wt%) were obtained from Honeywell Fluka. Deionized (DI) water was obtained using a Millipore filter system MilliQ®. The multi element anion standard solution for ion chromatography was obtained from Carl Roth GmbH + Co.KG. Na_2CO_3 and $NaHCO_3$ (>99% purity) were obtained from Sigma-Aldrich. The mass of [P_{44414}]Cl, water and acid solution additions were measured using an analytical balance (Precisa gravimetries AG, within ±0.0001 g). The IL cation, $[P_{44414}]^+$, was quantified with NMR (Bruker Avance III, 400 Hz and ±5%) using benzene as internal standard. The $[P_{44414}]^+$ cation concentration was calculated using the integration of the ^{1}H NMR spectral peaks. The concentration of H^+ was obtained from acid–base titrations (Titroline 6000 pH meter; ±0.1%) and the water content using Karl Fischer (Titroline 7500 KF Trace; ±0.15%).

Phase diagrams and tie-lines

Binodal curves were obtained by the cloud point titration method[16] at different temperatures. A known mass of IL was inserted into a glass vessel, and mixed with water until a clear mixture was obtained. The temperature of the glass vessel was controlled with circulation of water at constant temperature and the precision was verified within ±0.1 °C. An acid solution of known concentration was added drop wise to the mixture until the turbidity was observed. Addition of a known mass of water made the solution clear again, and this procedure was repeated several times. Binodal data were calculated using the mass of each component added. The amount of water added by use of acidic aqueous solutions (37 wt%, 96 wt% and 68 wt% for HCl, H_2SO_4 and HNO_3, respectively) was taken into account in this calculation.

Tie-lines were determined by an analytical method. Three mixture points in the biphasic region of the phase diagram HCl–[P_{44414}]Cl–H_2O were selected and prepared gravimetrically by mixing appropriate amounts of IL, acid and water. The mixtures were agitated and left overnight with temperature control at 25 and 50 °C, and the coexisting phases were carefully separated and weighed for their analyses. In the system HCl–[P_{44414}]Cl–H_2O, the anion was common to both IL and acid. Henceforth, the IL cation and H^+ concentrations are mentioned as IL and HCl concentrations, respectively. The complete chemical composition was obtained (IL, HCl and H_2O) for both phases and these data were used to draw tie-lines, connecting the upper and lower phase composition. The tie-line length (TLL) at different compositions and temperatures was calculated using eqn (1).

$$\mathrm{TLL} = [(Y_u - Y_l)^2 + (X_u - X_l)^2]^{1/2} \quad (1)$$

where Y and X are the mass fractions of IL and acid, respectively, and the subscripts u and l represent the upper and lower phases, respectively.

Ion exchange

Three mixture points were selected in the biphasic region of the HNO_3–[P_{44414}]Cl–H_2O and H_2SO_4–[P_{44414}]Cl–H_2O phase diagrams and prepared gravimetrically by mixing appropriate amounts of IL, acid and water. The mixtures were agitated and left overnight at 25 °C and the coexisting phases were carefully separated and weighed for their analyses. The $[P_{44414}]^+$ cation and H^+ were quantified using NMR and conventional acid–base titration. Chlorides and sulfates were quantified with ion chromatography (Metrohm, Metrosep A supp 15-250/40 anion column) for lower phases, while the amount of chlorides and sulfates present in upper phases was deduced from mass balance and electroneutrality of each phase. A mixture of Na_2CO_3 (0.7 mM) and $NaHCO_3$ (1.7 mM) was used as an eluent for this anion column.

Results and discussion

Simple AcABS: HCl–[P_{44414}]Cl–H_2O

The simplest IL-based AcABS is composed of an acid and an IL sharing a common anion – HCl and [P_{44414}]Cl – and water. In this case, the number of different individual moieties is kept to a minimum of four: three ions and H_2O as the only neutral species, assuming no ionic association takes place, whatever the ionic strength of the system. In the following, this AcABS will be thus considered as a quaternary system instead of a usual ternary system. The latter focuses on the practical aspects, pointing that a minimum of three chemical compounds is needed to prepare the mixtures, while our categorization emphasizes individual interactions between species.

The phase diagrams of HCl–[P_{44414}]Cl–H_2O system at different temperatures (T = 8, 13, 16, 25, 36, 45, 50 and 56 °C) were determined experimentally and are depicted in Fig. 1 in both 2D and 3D representations. The detailed experimental data for the binodal curves are reported in the Tables S1 and S2 of the ESI.† In Fig. 1a (2D representation) the monophasic region is located to the left of the binodal curves, while biphasic region exists to the right. Since the concentrated HCl solution contains only 37 wt% of acid at 25 °C due to the limited extent of HCl gas solubility in water, the dashed line represented on Fig. 1a gives the limit of the experimentally reachable region with the chemicals used.

The binodal curves of HCl–[P_{44414}]Cl–H_2O system evidence a very strong temperature dependency above 25 °C (*cf.* Fig. 1a). This strong temperature dependency of the system allows for the separation of metals from a large range of leachate solutions with different acid concentrations, greatly increasing the applicability of AcABS. However, no temperature effect is observed below 25 °C, with all binodal curves at 25, 16, 13 and 8 °C overlapping. Thus, these curves are not represented in Fig. 1 for the sake of clarity. The binodal curves at 25, 16, 13 and 8 °C are represented in Fig. S1 of the ESI.†

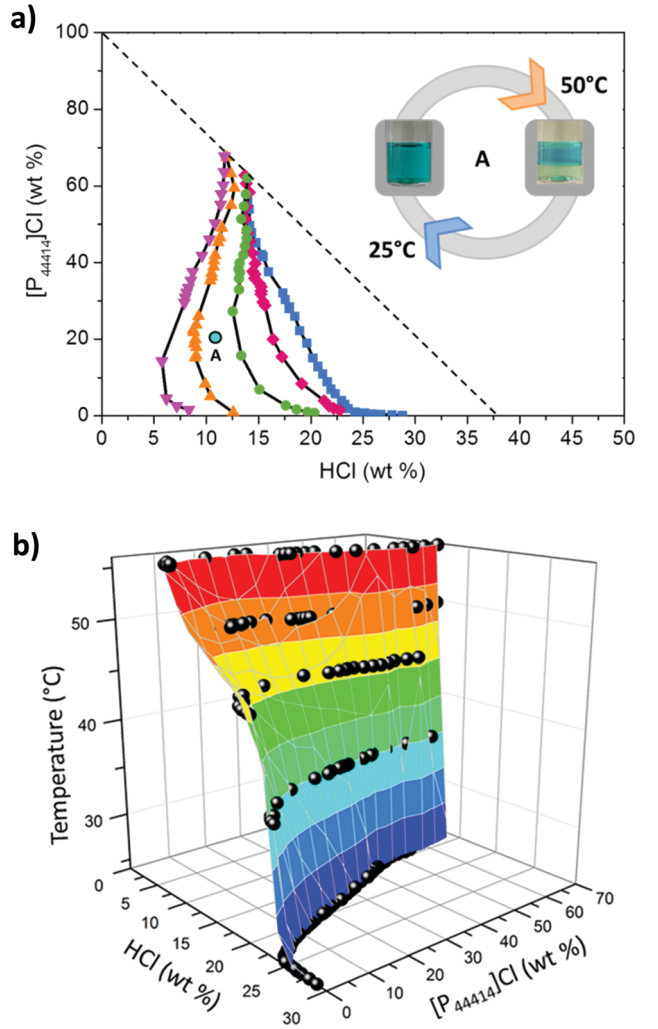

Fig. 1 The temperature effect on the phase diagrams of HCl–[P_{44414}]Cl–H_2O. (a) 2D representation of the binodal curves at 25 °C (■), 36 °C (◆), 45 °C (●), 50 °C (▲) and 56 °C (▼); illustration of phase behavior for the mixture point of composition A (11.5 wt% acid; 20 wt% IL; 68.5 wt% H_2O) at 25 and 50 °C; metal solutions were used for visual distinction of phases. (b) 3D representation of the temperature effect on the phase diagrams of HCl–[P_{44414}]Cl–H_2O in the temperature range 25 to 56 °C.

A closer analysis of the binodals of HCl–[P_{44414}]Cl–H_2O system indicates the presence of two different domains: (i) a temperature dependent domain for [P_{44414}]Cl concentration below 50 wt% and (ii) a temperature independent one for [P_{44414}]Cl concentration above 50 wt%. In the first domain, the temperature dependency is rather sharp as binodal curves obtained for *ca.* 5 °C intervals are well separated. As illustrated in Fig. 1a for the mixture point A, at temperatures above 25 °C the system could be either monophasic or biphasic depending on the temperature, being possible to induce reversible phase transitions by small changes in temperature. The biphasic region of HCl–[P_{44414}]Cl–H_2O system is favored by the increase of temperature. That is, for a given amount of ionic liquid, less HCl is required to induce an ABS at higher temperatures. In fact, contradictory to many IL-based ABS which exhibit an upper critical solution temperature (UCST) behavior, the LCST behaviour is a defining feature of phosphonium-based ILs with a cation equal to or larger than $[P_{4444}]^+$.[17–20] The situation is quite different above 50 wt% of IL, as all binodal curves merge. This indicates that as the IL wt% increases, the impact of temperature on the binodal is less important. These results can be explained by the hydrophilicity of [P_{44414}]Cl being temperature dependent, a behavior similar to what is observed for PEG and other non-ionic surfactants.[21] The onion shape of the higher temperature binodals is also uncommon. The only example of IL-based ABS binodals with a similar shape was reported by Neves *et al.*[22] Other such odd curves were observed in PEG–salt ABS systems by Graber *et al.*[23] and Sadeghi *et al.*[24]

Interestingly, this so-called onion shape reveals the possibility to revert to monophasic region from a biphasic region when the concentration of ionic liquid increases. For example, at T = 50 °C, for a point (12 wt% HCl, 10 wt% IL and 78 wt% of H_2O), the mixture is biphasic. Addition of large amounts of IL (~30 wt%) to the above mixture leads to the formation of monophasic state, a phenomenon that is not expected in such systems.

Correlation of binodal curves with empirical equations

Once the binodal curve is experimentally obtained, it is important to determine the exact composition of the upper and bottom phases. To this purpose, in order to avoid lengthy and minute analytical protocols, and based on a method first proposed by Merchuk *et al.*,[25] the lever-arm rule is commonly used together with an empirical fit of the experimental binodal.[26] The most used empirical equation to fit binodal curves is the so-called Merchuk equation.[25] However, several other equations have been proposed that are gathered in Table 1.[23,27–33] These mathematical expressions, with a number of fitting parameters ranging from three to five, attempt at describe a smooth decreasing experimental data set, as binodal curves tend to have that shape. To the best of our knowledge, there is no theoretical analytical description of such binodal curves.

Table 1 Representation of empirical equations to fit binodals from literature

No.	Equation	Ref.
(2)	$w_1 = a\exp[(bw_2^{0.5}) - (cw_2^3)] -$ Merchuk equation	25 and 27
(3)	$w_1 = a + bw_2^{0.5} + cw_2 + dw_2^2$	28
(4)	$w_1 = a\ln(w_2 + c) + b$	29
(5)	$w_1 = a + bw_2^{0.5} + cw_2$	30
(6)	$\frac{1}{w_1} = a + bw_2^{0.5} + cw_2$	23
(7)	$w_1 = -\ln\left(V_{213^*}\frac{w_2}{M_2}\right)\frac{M_1}{V_{213^*}}$	31
(8)	$w_1 = a + bw_2^{0.5} + cw_2 + dw_2^2 + ew_2^3$	32
(9)	$w_1 = a\exp\left(-\frac{w_2}{b}\right) + c\exp\left(-\frac{w_2}{d}\right) + e$	33

w_1 and w_2 represent the mass fractions of the upper and lower phases, respectively, and a, b, c, d, e are the fitted parameters. In eqn (6), the parameters V_{213}*, M_1 and M_2 are the excluded volume of salt, and the molar mass of polymer and salt, respectively.

In the present case, the binodals' onion-shape (*cf.* Fig. 1a) makes experimental binodal fitting difficult. At temperatures higher than 45 °C, for a single value on *x*-axis (HCl wt%), two values of IL wt% correspond to the binodal curve. As an example, in Fig. 1a is possible to see that the binodal curve at 56 °C exhibits two IL concentrations equal to 1.6 and 33.4 for the same concentration of HCl of 8.3 wt%. Mathematically speaking, this corresponds to a non-injective experimental function. Hence, the traditional fitting of experimental binodal curves using any of the proposed empirical equations, and at the first place, the Merchuk equation, is unable to recover the data.

This could be solved by plotting the curves along other axes, where the experimental functions are injective, and probably be described by one or more empirical equations present in Table 1.

These uncommon curve plots and fittings have already been executed by various authors with polymers on *x*-axis and salts on *y*-axis.[23,24] The experimental binodal data at 25 °C and 50 °C were plotted in different combinations and were fitted with all the equations given in Table 1, with eqn (3) giving the best fit for all the workable plot combinations, although these plots look very different at the first sight. The viable plot combinations for 25 °C and 50 °C and equation coefficient values are represented in Table 2 along with respective standard deviations (σ^2). The plot combinations HCl = f([P_{44414}]Cl) and H_2O = f([P_{44414}]Cl) gave the lowest χ^2 values at 25 °C and 50 °C (0.0764 and 0.0625 respectively). Fig. 2 shows the binodal fitting for the plot HCl = f([P_{44414}]Cl) at 25 °C and 50 °C.

Plotting HCl on *y*-axis and IL on *x*-axis is special, while plotting H_2O on *y*-axis and IL on *x*-axis is unique as the usual representation corresponds to the upper phase on *y*-axis and lower phase on *x*-axis.[10,26,34]

Tie-lines of HCl–[P_{44414}]Cl–H_2O system

The tie-lines of HCl–[P_{44414}]Cl–H_2O system were determined analytically, and the TLLs calculated by eqn (1). The weight percentage compositions, phase volumes, and TLL of each tie-line are reported in Table 3. Fig. 3 illustrates the tie-lines of three mixture points B, C and D that were prepared in such a way that the wt% of the IL remains constant while HCl concentration varies for each point, allowing the evaluation of the acid effect on their behavior. Temperature effect was also considered by measuring the tie-lines at 25 and 50 °C.

The tie-line ends of a phase mixture represent the compositions of both upper and lower phases on the binodal curve at a given temperature. As mentioned in the previous section, the preparation of binodal points at IL and HCl concentrations above the limit depicted as a dash-dot black line in Fig. 3 is impossible using 37 wt% HCl. However, at 50 °C, the composition of the upper phase arising from preparation of sample D appears to belong to the "forbidden region". This apparent paradox is a direct consequence of the formation mechanism of AcABS, as already discussed by Gras *et al.*[13] As the temperature is raised, water and HCl are excluded from the upper phase, thus leading to dehydration of this phase and, consequently obtaining an IL amount above the limit allowed by direct use of HCl at 37 wt%. Thus, tie-lines could be used as a method to determine the binodal curves at higher concentrations of IL, which otherwise is not reachable. In most cases, the tie-lines do not seem to cross the starting mixture points. This is due to the experimental uncertainty of ±5 wt% in the measurement of the compositions of the phases in equilibrium.

At 25 °C, for point B, IL is mainly present in the upper phase while the HCl is almost equally distributed between the two phases, with 40% of the total HCl present in the upper phase and the remaining in the lower phase, which has only a minor amount of IL. As the mixture points move away from the binodal, points C and D, the IL is concentrated in the upper phase, with a negligible content (<0.30 wt%) in the lower

Table 2 Coefficients for the best fitted equation (eqn (3)) of binodal data at two different temperatures, T = 25 °C and 50 °C

Temperature	Plot combinations	*A*	*B*	*C*	*D*	Standard dev.[a]
T = 25 °C	HCl = f([P_{44414}]Cl)	28.40	−3.123	0.286	-2.55×10^{-3}	0.0764
T = 25 °C	[P_{44414}]Cl = f(HCl)	−370.6	352.6	−74.76	0.762	0.1830
T = 25 °C	H_2O = f(HCl)	472.6	−353.8	73.94	−0.764	0.1830
T = 25 °C	H_2O = f([P_{44414}]Cl)	71.6	3.124	−1.287	2.55×10^{-2}	0.0764
T = 50 °C	HCl = f([P_{44414}]Cl)	15.867	−3.666	0.5333	-0.202×10^{-2}	0.0625
T = 50 °C	HCl = f(H_2O)	−49.731	26.479	−3.0771	0.0107	0.0793
T = 50 °C	[P_{44414}]Cl = f(H_2O)	149.29	−26.303	2.0578	-1.07×10^{-2}	0.0793
T = 50 °C	H_2O = f([P_{44414}]Cl)	84.132	3.666	−1.533	2.02×10^{-3}	0.0625

[a] Standard deviation = $\frac{1}{N}\sum_{i=1}^{N}\sqrt{\left(w_1^{\exp} - w_1^{\text{cal}}\right)^2}$.

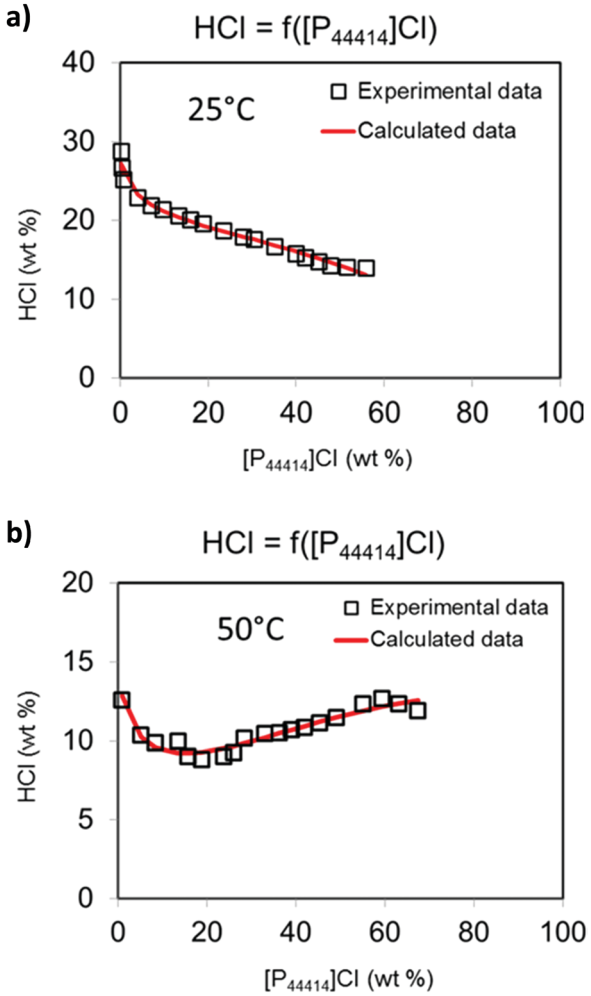

Fig. 2 Fitting of HCl–[P_{44414}]Cl–H_2O binodal curve experimental data at (a) 25 °C and (b) 50 °C for HCl = *f* ([P_{44414}]Cl).

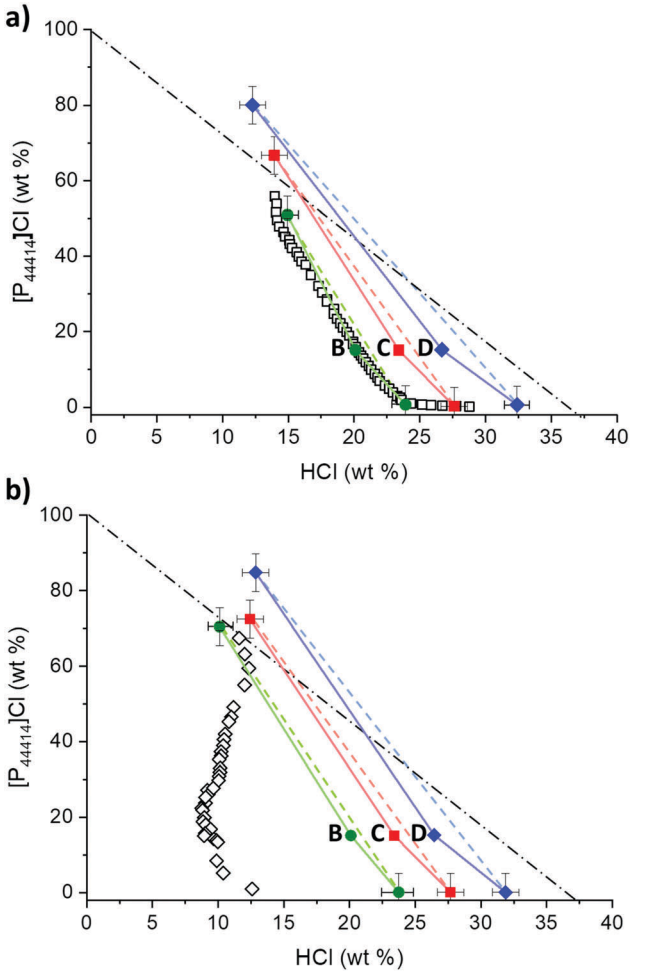

Fig. 3 Representation of the tie-lines for the ternary system HCl–[P_{44414}]Cl–H_2O at (a) 25 °C and (b) 50 °C.

Table 3 Weight percent compositions for TLs and respective TLLs of HCl–[P_{44414}]Cl–H_2O ABS, in the upper (u) and lower (l) phases and the initial biphasic composition of the mixture (M) at 25 and 50 °C, and at atmospheric pressure

		Weight percent composition (wt%)						% of initial volume		
T (°C)	Mixture points	HCl_M	IL_M	HCl_u	IL_u	HCl_l	IL_l	% V_u	% V_l	TLL
25 °C	B	20.1	15.1	14.9	50.9	23.9	0.69	34.0	66.0	51.0
	C	23.4	15.1	13.9	66.7	27.6	0.28	27.9	72.1	67.8
	D	26.7	15.2	12.3	80.0	32.4	0.06	25.0	75.0	81.9
50 °C	B	20.4	15.1	10.1	70.4	23.7	0.05	23.5	76.5	71.7
	C	23.4	15.1	12.4	72.4	27.7	0.04	24.0	76.0	74.0
	D	26.4	15.3	12.8	84.8	31.9	0.05	22.6	77.4	86.8

phase. In these mixtures, the acid is mainly present in the lower phase, with concentrations <15 wt% in the upper phase. Phase volumes also vary significantly from points B to D where a decrease in the upper (IL-rich) phase volume is observed.

At 50 °C, for all the mixture points, the IL is essentially depleted from the lower (acid-rich) phase with concentrations ≤0.05 wt%, while the HCl partitions between the two phases, with less than 30% of total HCl in the upper phase and more than 70% in the lower phase. The volumes of upper phases are smaller than those obtained at 25 °C. Furthermore, the TLLs increase with temperature for all mixture points due to the increase of the biphasic region. As described earlier, a very important character of this system is that when the phases are separated, the upper phase contains essentially all the IL with some HCl, whereas the lower phase is essentially an aqueous solution of the acid. This is very interesting for extraction applications, where the IL can successfully extract the products of interest without loss to the lower phase, while the acidic solution can be recovered more concentrated than the feed solution.

Towards more complex IL-based AcABS: HNO_3/H_2SO_4–[P_{44414}]Cl–H_2O systems

If the acid and salt do not share a common ion, the number of species in the system increases when compared to the simple HCl–[P_{44414}]Cl–H_2O system. Ion exchange can occur in systems with divergent ions when the two compounds come into contact in aqueous solution. Depending upon the type of IL/acid system used and the desired objective, ion exchange could be helpful or undesirable.

As discussed earlier, in HCl–[P_{44414}]Cl–H_2O system the IL cation is essentially present in the upper phase and negligible amounts of $[P_{44414}]^+$ are found in the lower phase, meaning that in this AcABS the ion exchange could only occur on the anion. Thus, in order to study the ion exchange in this type of systems, more complex AcABS composed of HNO_3 or H_2SO_4 were considered. The number of species present in these systems fortunately does not prevent to plot a phase diagram, which is obtained with H_2O, nitric or sulfuric acid and [P_{44414}]Cl as starting chemicals. For the sake of comparison and because acids have different molecular weights, the corresponding binodal curves are displayed in Fig. 4 in molality (mol kg^{-1} of solvent). Note that in wt% units binodals obtained with H_2SO_4 or HCl, for instance, overlap. The detailed data for the binodal curves both in mol kg^{-1} and wt% units is reported in ESI,† Table S3.

Fig. 4 reveals that for the same amount of IL, the quantity of acid required to induce an ABS vary widely. In the case of H_2SO_4, the lowest concentration necessary to observe a phase separation is approximately 2 mol kg^{-1}. Because the pK_a of HSO_4^-/SO_4^{2-} is 1.7, H_2SO_4 is mainly dissociated as H^+ and HSO_4^- with formation of a small amount of SO_4^{2-} for mixtures close to the binodal.[35] Thus the H_2SO_4–[P_{44414}]Cl–H_2O system is a multicomponent senary system (H^+, P_{44414}^+, SO_4^{2-}, HSO_4^-, Cl^- and H_2O). Similarly, a biphasic state is obtained already above 0.5 mol kg^{-1} of HNO_3 and because HNO_3 is known to associate only above 3 mol kg^{-1} in water,[35] the HNO_3–P_{44414}Cl–H_2O system at the binodal should be considered a quinary system (H^+, P_{44414}^+, NO_3^-, Cl^- and H_2O).

The order of the acids concerning their ability to induce an AcABS is as follows: $HNO_3 > H_2SO_4 > HCl$ (*cf.* Fig. 4). Since the cation is common to all acids used, the AcABS formation efficiency depends on the acid anion. Therefore, this order demonstrates that the efficiency of nitrates to form an AcABS is higher than those of sulfates and chlorides. The established trend for the anions ($NO_3^- > SO_4^{2-} > Cl^-$) does not apparently follow the Hofmeister series.

Nevertheless, one should notice that due to the concentration of sulfuric acid used in this study, the predominant anion is HSO_4^-, and not SO_4^{2-}. This anion HSO_4^- has not been placed yet in the Hofmeister series because it is uncommon in aqueous solutions of neutral pH. Because all previous papers dealing with the formation of ABS have so far, reported that these systems followed the Hofmeister series, one can expect that HSO_4^- should lie between NO_3^- and Cl.

Such a proposal can be further pursued by studying the anion exchange mechanisms of the two systems: HNO_3–[P_{44414}]Cl–H_2O and H_2SO_4–P_{44414}Cl–H_2O. In the heavily ion-loaded phases of the systems studied here, the ionic compounds will dissociate, if only partly, upon mixing. Thus, the IL cation does not necessarily remain with the IL anion during the phase separation and, similarly, the H^+ is not required to follow the counter-anion with which it was introduced into the system, leading to potentially complex ion exchanges, the extent of which should be established to understand and characterize the AcABS. In the HNO_3–[P_{44414}]Cl–H_2O system, HNO_3 dissociates into H^+ and NO_3^- and the ion exchange could be described by eqn (10), whereas in H_2SO_4–[P_{44414}]Cl–H_2O system, H_2SO_4 being a weak mineral acid can dissociate into H^+, HSO_4^- and SO_4^{2-} ions. Thus, two types of anion exchanges might be possible with the IL anion – eqn (11) and (12).

$$[P_{44414}]Cl + H^+ + NO_3^- \rightarrow [P_{44414}]NO_3 + H^+ + Cl^- \quad (10)$$

$$[P_{44414}]Cl + H^+ + HSO_4^- \rightarrow [P_{44414}]HSO_4 + H^+ + Cl^- \quad (11)$$

$$2([P_{44414}]Cl) + 2H^+ + SO_4^{2-} \rightarrow [P_{44414}]_2SO_4 + 2H^+ + 2Cl^- \quad (12)$$

The mixture points E, F and G and H, I, and J were prepared in the biphasic region of the HNO_3–[P_{44414}]Cl–H_2O and H_2SO_4–[P_{44414}]Cl–H_2O systems respectively, with variable mole ratio of IL : acid (1 : 2, 1 : 5 and 1 : 20) as displayed in Fig. 4. Composition analyses of the upper and lower phases allows the quantification of each ion ($[P_{44414}]^+$, Cl^-, NO_3^-, HSO_4^-, SO_4^{2-} and H^+) present in these systems and the quantification of the ion-exchange extent. Table 4 reports the residual percentage of total moles of $[P_{44414}]^+$ cation and Cl^- anion with an error of ± 5% present in the upper phase after contacting with HNO_3 or H_2SO_4. The detailed experimental data is presented in Tables S4 and S5 of the ESI.†

In the H_2SO_4–[P_{44414}]Cl–H_2O system, the anion exchange is present in all the mixtures, although to a lesser extent than for the HNO_3 system, in line with the greater hydrophilicity of sulfate-based anions. The extent of exchange is dependent on the IL : acid ratio, with a decrease as the IL : acid ratio is reduced (point H). In the HNO_3–[P_{44414}]Cl–H_2O system, close to quantitative anion exchange is observed for the points F and G, where nitrates of acid exchange with Cl^- ions of IL. In mixture point E, with higher IL concentration compared to the other two mixture points, the exchange is slightly lower, leaving 37% of chloride anions with the $[P_{44414}]^+$ cation. These results show that the anion exchange is extensive in all cases. Because electroneutrality needs to be respected, nitrates originating from the acid are present in the upper phase with the IL, Cl^- anions migrating to the aqueous phase. This results in a novel IL, [P_{44414}][NO_3], present in the upper phase of the AcABS. Note that this phenomenon could be described as a simple metathesis

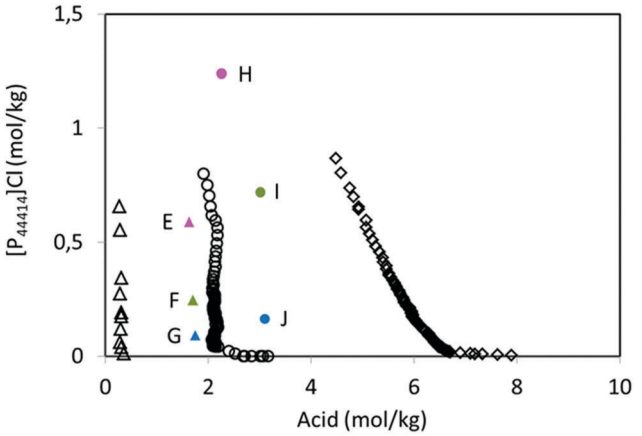

Fig. 4 Phase diagrams of AcABS composed of [P_{44414}]Cl, water and the acids HCl (◊), H_2SO_4 (○) and HNO_3 (△). The mixture points E, F and G belong to HNO_3-based system and H, I and J to H_2SO_4-based system.

Table 4 Residual percentage of total moles (±5%) of $[P_{44414}]^+$ cation and Cl^- anion present in the upper phase after contacting with HNO_3 or H_2SO_4 in the HNO_3–$[P_{44414}]Cl$–H_2O and H_2SO_4–$[P_{44414}]Cl$–H_2O systems

Mixture points (HNO_3/H_2SO_4)	HNO_3 system		H_2SO_4 system	
IL : acid ratio	% Cl^-	% $[P_{44414}]^+$	% Cl^-	% $[P_{44414}]^+$
E/H = 1 : 2	36.6	100.0	83.6	95.9
F/I = 1 : 5	4.4	97.8	51.2	92.6
G/J = 1 : 20	1.9	100.0	16.4	73.1

procedure in order to produce $[P_{44414}][NO_3]$ starting from $[P_{44414}]Cl$ and HNO_3. This explains the unexpected high ability of HNO_3 to form AcABS, as the resulting $[P_{44414}][NO_3]$ IL is hydrophobic.

The results obtained for NO_3^- and Cl^- are in perfect agreement with a recent publication[14] that demonstrates that in the case of a metathesis procedure carried out using $[P_{66614}]NO_3$ and various anions, including Cl^-, the anion exchange occurs following the Hofmeister series. That is, $[P_{66614}]NO_3$ did not yield any anion exchange when contacted with a chloride salt. In our case, $[P_{44414}]Cl$ contacted with HNO_3 yields an efficient anion exchange. Considering the similarity between $[P_{44414}]^+$ and $[P_{66614}]^+$ cations, our results clearly agree with this report. Similarly, when $[P_{44414}]Cl$ is mixed with H_2SO_4, anion exchange occurs, however less pronounced than that observed using HNO_3.

Finally, upon preparing a mixture containing 26.6 and 36.5 wt% $[P_{44414}]HSO_4$ and HNO_3, two phases appear. Analysis of the partition of the HSO_4^- anions between the two phases reveal that HSO_4^- is indeed present in both phases, implying some anion exchange between NO_3^- and HSO_4^-. This tends to further confirm the previous assumption that HSO_4^- can be implemented in the Hofmeister series as follows: $NO_3^- > HSO_4^- > Cl^-$, and that these AcABS, as other classical ABS, follow this series. These results also show that such phenomenon, when occurring can have a dramatic impact on the hydrophobicity of ILs and consequently, on the phase separation of aqueous biphasic systems.

The ion exchange shown above raises a question regarding the possibilities of obtaining the composition of a biphasic mixture from a binodal curve such as those presented in Fig. 4 using any empirical equation and the lever-arm rule. For instance, the fact that ion exchange occurs implies that at equilibrium, the lower phase of HNO_3–$[P_{44414}]Cl$–H_2O and H_2SO_4–$[P_{44414}]Cl$–H_2O is an aqueous solution of HCl and HNO_3 or H_2SO_4, accordingly. When ion exchange occurs, there is a discrepancy between the apparent phase diagram, the corresponding tie-lines and the true compositions of the phases of an ABS.

Conclusion

Phase diagrams corresponding to the HCl–$[P_{44414}]Cl$–H_2O aqueous biphasic system at various temperatures highlight the thermoreversible behavior, with an increase in temperature driving the biphasic formation. The high temperature impact on the binodals allows the development of thermoresponsive systems in which the required acid concentration to form an AcABS is drastically reduced. The fitting of these unique binodal curves demonstrates that the Merchuk equation does not apply in these cases. The tie-lines of the HCl–$[P_{44414}]Cl$–H_2O system were thus analytically determined using various analytical methods. The AcABS systems in which the IL and the acid share a common anion, namely HCl–$[P_{44414}]Cl$–H_2O system, minimize the loss of IL to the aqueous phase thereby ensuring quantitative partition of the IL to the IL-rich phase. Studying the effect of other acids on the $[P_{44414}]Cl$-based AcABS, the binodal curves of $[P_{44414}]Cl$ with HNO_3 and H_2SO_4 are a direct result of anion-exchange between the chloride anion of the IL and that of the inorganic acid. A high degree of anion exchange was present in both the HNO_3/H_2SO_4–$[P_{44414}]Cl$–H_2O systems and the percentage of exchange depends on the type of acid and IL concentration used. Thus, such a versatile AcABS can be tuned accordingly to produce two different ILs by inducing an anion exchange or recovering the initial IL by keeping a common cation. The preliminary results of IL-based AcABS indicate their tunable and flexible characteristics which are promising for various industrial applications.

Conflicts of interest

There are no conflicts to declare.

Acknowledgements

This work was part of BATRE-ARES project (ERAMIN/0001/2015) funded by ADEME and FCT. Matthieu Gras would like to acknowledge labex CEMAM for financial support. This work was partly developed in the scope of the project CICECO – Aveiro Institute of Materials, POCI-01-0145-FEDER-007679 (FCT Ref. UID/CTM/50011/2013).

References

1 P. A. Albertsson, *Partition of Cell Particles and Macromolecules*, Wiley-VCH, Weinheim, 1962.
2 J. A. Asenjo and B. A. Andrews, *J. Chromatogr. A*, 2011, **1218**, 8826–8835.
3 Y. Liu, Y. Feng and J. Lun, *Food Bioprod. Process.*, 2012, **90**, 111–117.
4 K. E. Gutowski, G. A. Broker, H. D. Willauer, J. G. Huddleston, R. P. Swatloski, J. D. Holbrey and R. D. Rogers, *J. Am. Chem. Soc.*, 2003, **125**, 6632–6633.
5 M. G. Freire, *Ionic-Liquid-Based Aqueous Biphasic Systems – Fundamentals*, Springer, Berlin, Heidelberg, 2016.
6 A. F. M. Cláudio, A. M. Ferreira, S. Shahriari, M. G. Freire and J. A. P. Coutinho, *J. Phys. Chem. B*, 2011, **115**, 11145–11153.
7 S. P. M. Ventura, S. G. Sousa, L. S. Serafim, Á. S. Lima, M. G. Freire and J. A. P. Coutinho, *J. Chem. Eng. Data*, 2012, **57**, 507–512.
8 M. G. Freire, A. F. M. Cláudio, J. M. M. Araújo, J. A. P. Coutinho, I. M. Marrucho, J. N. C. Lopes and L. P. N. Rebelo, *Chem. Soc. Rev.*, 2012, **41**, 4966–4995.

9 T. Shimomura and M. Sugiyama, *J. Chem. Eng. Data*, 2018, **63**, 402–408.
10 J. Gao, L. Chen and Z. Yan, *J. Chem. Eng. Data*, 2015, **60**, 464–470.
11 H. Passos, A. Luís, J. A. P. Coutinho and M. G. Freire, *Sci. Rep.*, 2016, **6**, 20276.
12 E. T. Fox, J. E. F. Weaver and W. A. Henderson, *J. Phys. Chem. C*, 2012, **116**, 5270–5274.
13 M. Gras, N. Papaiconomou, N. Schaeffer, E. Chainet, F. Tedjar, J. A. P. Coutinho and I. Billard, *Angew. Chem., Int. Ed.*, 2018, **57**, 1563.
14 D. Dupont, D. Depuydt and K. Binnemans, *J. Phys. Chem. B*, 2015, **119**, 6747–6757.
15 K. E. Gutowski, G. A. Broker, H. D. Willauer, J. G. Huddleston, R. P. Swatloski, J. D. Holbrey and R. D. Rogers, *J. Am. Chem. Soc.*, 2003, **125**, 6632–6633.
16 C. M. S. S. Neves, S. P. M. Ventura, M. G. Freire, I. M. Marrucho and J. A. P. Coutinho, *J. Phys. Chem. B*, 2009, **113**, 5194–5199.
17 S. Saita, Y. Kohno and H. Ohno, *Chem. Commun.*, 2013, **49**, 93–95.
18 R. Wang, W. Leng, Y. Gao and L. Yu, *RSC Adv.*, 2014, **4**, 14055–14062.
19 A. Nitta, T. Morita, S. Saita, Y. Kohno, H. Ohno and K. Nishikawa, *Chem. Phys. Lett.*, 2015, **628**, 108–112.
20 B. Dong, X. Xing, R. Wang, B. Wang, X. Zhou, C. Wang, L. Yu, Z. Wu and Y. Gao, *Chem. Commun.*, 2015, **51**, 11119–11122.
21 B. Lindman, B. Medronho and G. Karlström, *Curr. Opin. Colloid Interface Sci.*, 2016, **22**, 23–29.
22 C. M. S. S. Neves, S. P. M. Ventura, M. G. Freire, I. M. Marrucho and J. A. P. Coutinho, *J. Phys. Chem. B*, 2009, **113**, 5194–5199.
23 T. A. Graber, M. E. Taboada, J. A. Asenjo and B. A. Andrews, *J. Chem. Eng. Data*, 2001, **46**, 765–768.
24 R. Sadeghi and F. Jahani, *J. Phys. Chem. B*, 2012, **116**, 5234–5241.
25 J. C. Merchuk, B. A. Andrews and J. A. Asenjo, *J. Chromatogr. B: Biomed. Sci. Appl.*, 1998, **711**, 285–293.
26 M. V. Quental, H. Passos, K. A. Kurnia, J. A. P. Coutinho and M. G. Freire, *J. Chem. Eng. Data*, 2015, **60**, 1674–1682.
27 S. L. Mistry, A. Kaul, J. C. Merchuk and J. A. Asenjo, *J. Chromatogr. A*, 1996, **741**, 151–163.
28 M. Hu, Q. Zhai, Y. Jiang, L. Jin and Z. Liu, *J. Chem. Eng. Data*, 2004, **49**, 1440–1443.
29 P. González-Tello, F. Camacho, G. Blázquez and F. J. Alarcón, *J. Chem. Eng. Data*, 1996, **41**, 1333–1336.
30 M. Jayapal, I. Regupathi and T. Murugesan, *J. Chem. Eng. Data*, 2007, **52**, 56–59.
31 D. Baskaran, K. Chinnappan, R. Manivasagan and R. Selvaraj, *J. Chem. Eng. Data*, 2017, **62**, 738–743.
32 Y. Zhang, S. Zhang, Y. Chen and J. Zhang, *Fluid Phase Equilib.*, 2007, **257**, 173–176.
33 X. Xie, Y. Yan, J. Han, Y. Wang, G. Yin and W. Guan, *J. Chem. Eng. Data*, 2010, **55**, 2857–2861.
34 C. M. S. S. Neves, S. Shahriari, J. Lemus, J. F. B. Pereira, M. G. Freire and J. A. P. Coutinho, *Phys. Chem. Chem. Phys.*, 2016, **18**, 20571–20582.
35 D. D. Perrin, *Ionisation Constants of Inorganic Acids and Bases in Aqueous Solution*, Elsevier, 2016.

